AD-A091 534 NORTHWESTERN UNIV EVANSTON IL DEPT OF CHEMISTRY F/G 7/4
BROMINE AS A PARTIAL OXIDANT. OXIDATION STATE AND CHARGE TRANSP--ETC(U)
OCT 80 D W KALINA, J W LYDING, M S MCCLURE N00014-77-C-0231
UNCLASSIFIED TR-13 NL

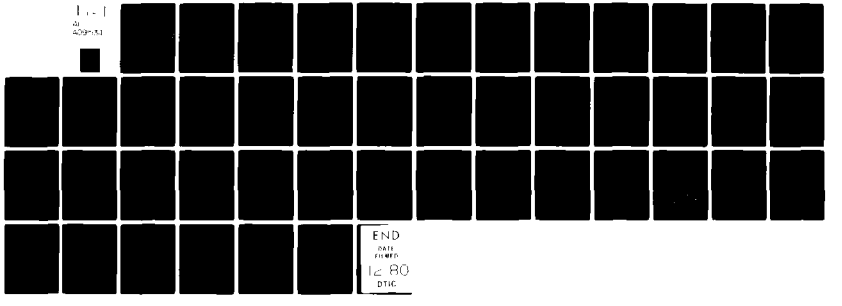

END
DATE FILMED
12-80
DTIC

OFFICE OF NAVAL RESEARCH
Contract N00014-77-C-0231
Task No. NR 053-640

TECHNICAL REPORT NO. 13

Bromine as a Partial Oxidant. Oxidation State and Charge Transport in Brominated Nickel and Palladium Bisdiphenylglyoximates. A Comparison with the Ionidated Materials and Resonance Raman Structure-Spectra Correlations for Polybromides

by

Davida W. Kalina, Joseph W. Lyding, Malcolm S. McClure, Carl R. Kannewurf and Tobin J. Marks

Prepared for Publication in

Journal of the American Chemical Society

Northwestern University
Department of Chemistry
Evanston, IL 60201

October 6, 1980

unclassified

SECURITY CLASSIFICATION OF THIS PAGE (When Data Entered)

REPORT DOCUMENTATION PAGE		READ INSTRUCTIONS BEFORE COMPLETING FORM
1. REPORT NUMBER Technical Report No. 13	2. GOVT ACCESSION NO. AD-A091 534	3. RECIPIENT'S CATALOG NUMBER
4. TITLE (and Subtitle) Bromine as a Partial Oxidant. Oxidation State and Charge Transport in Brominated Nickel and Palladium Bisdiphenylglyoximates. A Comparison with the Iodinated Materials and Resonance Raman Structure-Spectra Correlations for Polybromides.		5. TYPE OF REPORT & PERIOD COVERED 6. PERFORMING ORG. REPORT NUMBER
7. AUTHOR(s) Davida W. Kalina, Joseph W. Lyding, Malcolm S. McClure, Carl R. Kannewurf, and Tobin J. Marks.		8. CONTRACT OR GRANT NUMBER(s) N00014-77-C-0231
9. PERFORMING ORGANIZATION NAME AND ADDRESS Northwestern University Department of Chemistry Evanston, IL 60201		10. PROGRAM ELEMENT, PROJECT, TASK AREA & WORK UNIT NUMBERS NR-053-640
11. CONTROLLING OFFICE NAME AND ADDRESS		12. REPORT DATE October 6, 1980 13. NUMBER OF PAGES 39
14. MONITORING AGENCY NAME & ADDRESS(if different from Controlling Office)		15. SECURITY CLASS. (of this report) Unclassified 15a. DECLASSIFICATION/DOWNGRADING SCHEDULE

16. DISTRIBUTION STATEMENT (of this Report)

Approved for public release; distribution unlimited

17. DISTRIBUTION STATEMENT (of the abstract entered in Block 20, if different from Report)

18. SUPPLEMENTARY NOTES

19. KEY WORDS (Continue on reverse side if necessary and identify by block number)

Low-dimensional material
Bromine
Resonance Raman spectroscopy
Electrical conductivity
Partial oxidation

20. ABSTRACT (Continue on reverse side if necessary and identify by block number)

This paper presents an investigation of oxidation state and charge transport in the low-dimensional materials $Ni(dpg)_2Br_{1.0}$ and $Pd(dpg)_2Br_{1.1}$, dpg = diphenylglyoximato. Resonance Raman structure-spectra correlations are discussed for polybromides, and Br_5^- is assigned as the predominant halogen species in both of these materials. Thus, the $M(dpg)_2$ units are formally in fractional oxidation states of ca. +0.20(2) (M=Ni) and +0.22(2) (M=Pd). In the optical spectra of both materials, a broad transition at 500 nm is related to the

DD FORM 1 JAN 73 1473 EDITION OF 1 NOV 65 IS OBSOLETE
S/N 0102-014-6601 |

unclassified

SECURITY CLASSIFICATION OF THIS PAGE (When Data Entered)

.00015/OMEGA CM .00091/OMEGA CM

polybromide chains. Four-probe single crystal electrical conductivities (dc) in the stacking direction at 300° K are as high as 9.1×10^{-4} $(\Omega cm)^{-1}$ ($Ni(dpg)_2Br_{1.0}$) and 1.5×10^{-4} $(\Omega cm)^{-1}$ ($Pd(dpg)_2Br_{1.1}$). The conductivity is demonstrated to be thermally activated with activation energies of 0.33 and 0.21 eV, respectively. The transport properties of the brominated materials are found to be very similar to those of the related $M(dpg)_2I$ materials (M=Ni, Pd), a result contrary to expectations if the halogen chains were the major charge carrier.

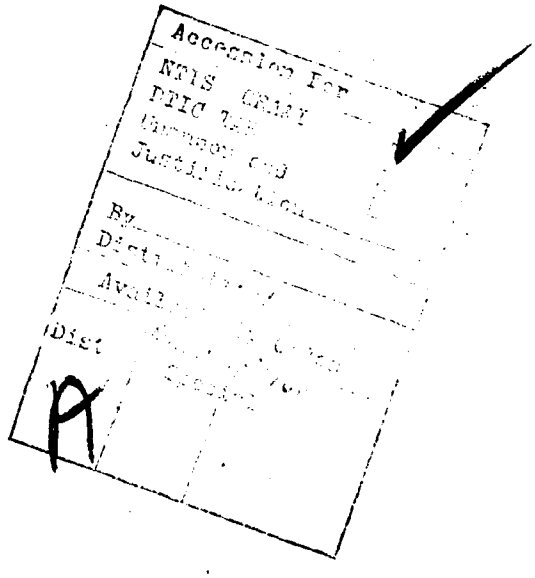

Contribution from the Department of
Chemistry, the Department of Electrical
Engineering and Computer Science, and
the Materials Research Center
Northwestern University
Evanston, Illinois 60201

BROMINE AS A PARTIAL OXIDANT. OXIDATION STATE AND CHARGE TRANSPORT IN BROMINATED NICKEL AND PALLADIUM BISDIPHENYLGLYOXIMATES. A COMPARISON WITH THE IODINATED MATERIALS AND RESONANCE RAMAN STRUCTURE-SPECTRA CORRELATIONS FOR POLYBROMIDES.

by Davida W. Kalina,[1a] Joseph W. Lyding,[1b] Malcolm S. Mc Clure,[1b]
Carl R. Kannewurf,*[1b] and Tobin J. Marks*[1a,c]

ABSTRACT

This paper presents an investigation of oxidation state and charge transport in the low-dimensional materials $Ni(dpg)_2Br_{1.6}$ and $Pd(dpg)_2Br_{1.1}$, dpg = diphenylglyoximato. Resonance Raman structure-spectra correlations are discussed for polybromides, and Br_5^- is assigned as the predominant halogen species in both of these materials. Thus, the $M(dpg)_2$ units are formally in fractional oxidation states of ca. +0.20(2) (M=Ni) and +0.22(2) (M=Pd). In the optical spectra of both materials, a broad transition at 500 nm is related to the polybromide chains. Four-probe single crystal electrical conductivities (dc) in the stacking direction at 300° K are as high as 9.1×10^{-4} $(\Omega\,cm)^{-1}$ ($Ni(dpg)_2Br_{1.0}$) and 1.5×10^{-4} $(\Omega\cdot cm)^{-1}$ ($Pd(dpg)_2Br_{1.1}$). The conductivity is demonstrated to be thermally activated with activation energies of 0.33 and 0.21 eV, respectively. The transport properties of the brominated materials are found to be very similar to those of the related $M(dpg)_2I$ materials (M=Ni,Pd), a result contrary to expectations if the halogen chains were the major charge carrier.

Solids exhibiting unusual low-dimensional, supermolecular cooperative phenomena have been the subject of intensive investigation in the past few years.[2] Concurrent emphasis has been placed upon developing rational synthetic routes to new materials, and upon developing the theoretical models needed to understand existing data as well as to guide future experiments. One successful approach to the synthesis of unidimensional, quasimetallic materials has been the partial oxidation by iodine[2,3] of stackable, conjugated, planar molecules having a certain selected range of ionization potentials.[3a] A rich variety of conductive mixed valent materials have been prepared from metallomacrocyclic precursors such as bisdiphenylglyoximates,[3,4] phthalocyanines,[3,5] dibenzotetraazaannulenes,[6] bisbenzoquinonedioximates,[3,7] and porphyrins;[8] highly conductive halogenated organic systems have included those derived from organochalcogenides such as tetrathiafulvalene[3,9] and tetrathiatetracene.[10,11] The structures of these types of materials invariably consist of stacks of mixed valent (partially oxidized) electron donors and chains of electron-accepting iodide or polyiodide counterions.[3a] A particular strength of the iodine oxidation procedure is that the form of the iodine (even if disordered) can be readily deduced from resonance Raman and iodine Mössbauer structure-spectra criteria.[3,12] Hence, if the stoichiometry is known, the actual degree of incomplete charge transfer can be readily determined.

Far less is known about the consequences of using bromine as an acceptor in the synthesis of low-dimensional mixed valent materials. With the exception of the TTF salts where halogen is present as I^- or Br^- and closely interacting with the positively charged donor units,[9d] there is little systematic information on how the degree of partial oxidation and charge transport facility vary with the nature of the halogen acceptor. Such questions bear upon those features which stabilize the mixed valence lattice (e.g., acceptor electron affinity[3a]) and the mechanism of charge transport. The latter issue concerns not only the possible

effects of acceptor screening, but also the actual pathway of conduction. Both donor stacks and polyhalide chains have been discussed as the primary conduction pathway in iodinated low-dimensional materials.[11,13,14] Finally, and unlike the case of polyiodides, there exists no systematic body of structure-spectra criteria which allow ready identification of polybromide structure, hence assessment of the degree of incomplete charge transfer for bromine-doped conductive materials.

We recently reported a detailed study of chemistry, spectroscopy, structure, oxidation state, and charge transport in iodinated nickel and palladium bisdiphenylglyoximates ($M(dpg)_2$, A).[4a] These materials are composed of stacks of partially oxidized, $M(dpg)_2^{+0.20}$ units and parallel chains of I_5^- counterions. The crystal structure of $Ni(dpg)_2I$ is shown in Figure 1. We now present a complementary investigation

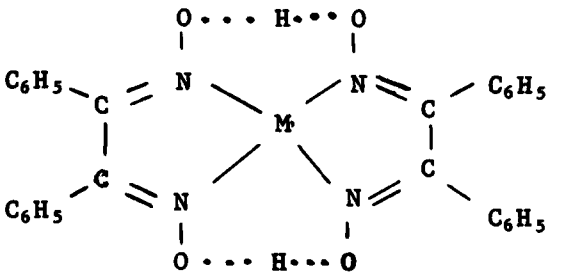

M = Ni, Pd

A

of the effect of substituting bromine for iodine in the $M(dpg)_2I$ materials. The bisdiphenylglyoximate systems are particularly attractive for halogen substitution studies since $M(dpg)_2Br$[4b,15,16] and $M(dpg)_2I$ are virtually isostructural (space group P4/ncc with nearly identical unit cell dimensions[16,17]). Furthermore, the halogen chain is spacially well-removed from the metal glyoximate core (ca. 7.2Å). We begin here by developing resonance Raman criteria for the elucidation of poly-

bromide structure, which, beyond the present system, should be useful in oxidation state characterization of a wide variety of bromine-doped electronic materials. Next, optical spectra are discussed and assigned. Finally, we focus in depth on the transport properties of the $M(dpg)_2I$ and $M(dpg)_2Br_x$ compounds. If the halogen chains are of primary importance in the conduction pathway, then an appreciable sensitivity of the transport characteristics to the identity of the halogen is expected.[18] It will be seen that single crystals of the brominated $M(dpg)_2$ materials are very similar to the iodinated materials in oxidation state and charge transport characteristics. This result implicates the $M(dpg)_2$ donor stacks as the major pathway for charge migration. A similar argument has recently been advanced in connection with $TTT_2I_xBr_{3-x}$ materials, but only <u>partial</u> replacement of iodine by bromine could be achieved;[11a] furthermore, the donor and acceptor molecules are not well-separated in the TTT-halogen system.[10c]

EXPERIMENTAL

All solvents and chemicals were reagent grade. The o-dichlorobenzene was dried over Davison 4A molecular sieves. Bis(diphenylglyoximato)nickel(II) and palladium(II) were prepared and purified as previously described.[4a] The $CsBr_3$[19a] and $(n\text{-}C_4H_9)_4N^+Br_3^-$ [19b] model compounds were prepared according to the literature procedures. Elemental analyses were performed by Ms. H. Beck, Northwestern Analytical Services Laboratory, Micro-Tech Laboratories, or Galbraith Laboratories. All brominated samples were stored in closed vials in a freezer at -20° C.

Synthesis of $Pd(dpg)_2Br_{1.1}$. This complex was prepared by reacting a gravity-filtered, o-dichlorobenzene solution of $Pd(dpg)_2$ (ca. 1.8×10^{-3} M) at 105° C with a ca. 24-fold molar excess of Br_2. The hot solution was allowed to cool to ambient temperature in the open atmosphere. Upon standing at room temperature for a period of 3-5 days, dark needle-like crystals were observed to settle from the solution. The lustrous reddish-brown crystals were collected by suction filtration and were washed with hexane until the washings were colorless. By this procedure, the yield of reddish-brown needles analyzing as $Pd(dpg)_2Br_{1.13(5)}$ was ca.40% . By doubling the concentration of $Pd(dpg)_2$ in the hot solution (ca. 3.6×10^{-3} M, ca. 12-fold molar excess of Br_2), a mixture of two different crystalline forms was obtained; the reddish-brown needles were present as well as brown parallelepipeds, analyzing as $Pd(dpg)_2Br_2 \cdot 2o\text{-}C_6H_4Cl_2$.

Anal. Calcd. for $Pd(C_{14}H_{11}O_2N_2)_2Br_{1.13}$ (reddish-brown needles): C, 49.81; H, 3.28; N, 8.30; Br, 13.37. Calcd. for $Pd(C_{14}H_{11}O_2N_2)_2Br_{1.00}$: C, 50.59; H, 3.34; N, 8.43; Br, 12.02. Found: C, 49.87; H, 3.31; N, 8.41; Br, 13.40 (average of three analyses). Calcd. for $Pd(C_{14}H_{11}O_2N_2)_2Br_2(o\text{-}C_6H_4Cl_2)_2$ (brown parallelepipeds): C, 46.25; H, 2.91; N, 5.39; Br, 15.39. Found: C, 46.25; h, 2.69; N, 5.44; Br, 17.49.

Infrared data for $Pd(dpg)_2Br_{1.1}$ (Nujol mull, cm^{-1}): 3075 w, 1970 vw, 1820 vw, 1595 mw, 1575 w, 1515 w, 1485 m, 1440 vs, 1335 m, 1300 s, 1275 m, 1150 m, 1140 m, 1070 w, 1025 m, 1000 w, 975 w, 925 mw, 880 s, 840 vw, 805 vw, 775 w, 765 s, 740 vs, 690 vs.

Synthesis of $Ni(dpg)_2Br_{1.0}$. This complex was prepared in a manner similar to that of $Pd(dpg)_2Br_{1.1}$. An o-dichlorobenzene solution of $Ni(dpg)_2$ (ca. 2.4×10^{-3} M) at 70° C was gravity filtered, rewarmed to 70° C, treated with a ca. 29-fold molar excess of Br_2, and allowed to cool to ambient temperature in the open atmosphere. Very small, brown, needle-like crystals possessing a metallic green luster formed immediately upon cooling. The crystals were collected by suction filtration and were washed with hexane until the washings were colorless. In this fashion, the yield of brown needles analyzing as $Ni(dpg)_2Br_{1.00(5)}$ was ca.45%. In attempts, similar to the technique used with the corresponding iodides,[4a] to obtain larger crystals by slowly cooling the hot o-dichlorobenzene solutions of $Ni(dpg)_2$ and Br_2, a white precipitate and very small amounts of a brown microcrystalline solid were recovered. Thus, $Ni(dpg)_2$ is decomposed when exposed to Br_2 at elevated temperatures for extended periods of time.

Anal. Calcd. for $Ni(C_{14}H_{11}O_2N_2)_2Br_{1.00}$: C, 54.50; H, 3.59; N, 9.08; Br, 12.95. Found: C, 54.30; H, 3.60; N, 8.97; Br, 12.94 (average of three analyses).

Infrared data for $Ni(dpg)_2Br_{1.0}$ (Nujol mull, cm^{-1}): 3075 w, 1970 vw, 1820 vw, 1600 mw, 1575 w, 1525 mw, 1490 s, 1445 vs, 1330 m, 1295 s, 1280 ms, 1155 m, 1140 vs, 1100 mw, 1070 mw, 1025 w, 1000 w, 975 mw, 930 m, 900 ms, 850 w, 770 s, 740 s, 690 vs, 670 mw, 388 m, 363 s, 320 ms, 298 s, 261 w, 173 vs, 110-140 s.

Raman Measurements. Laser Raman spectra were recorded with Ar^+(4579Å, 4880Å, 5145Å) excitation using a Spex 1401 monochromator and photon counting detection. The solid samples were studied in 5 or 12 mm Pyrex sample tubes spinning at 1200 rpm. A 180° back-scattering geometry was employed. A number of scans were made of each sample to check for possible sample decomposition. Spectra were calibrated with the exciting line (ν_o) or laser plasma lines.

Infrared Measurements. Routine infrared spectra were recorded with a Perkin-Elmer Model 267 spectrophotometer. Far-infrared spectra were obtained with a Perkin Elmer Model 180 instrument. Samples were studied as Nujol mulls between KBr or

polyethylene plates. The far-infrared studies were performed with a thorough and continuous purge of dry nitrogen.

Electronic Spectra. Spectra of solid samples were studied as Nujol mulls between quartz plates in a Cary 17-D spectrophotometer. Several scans were made of each sample to check for possible decomposition.

Electrical Conductivity Measurements. Temperature-dependent dc conductivity measurements were performed on single crystal specimens of $Ni(dpg)_2Br_{1.0}$ and $Pd(dpg)_2Br_{1.1}$ using an automated charge transport measurement system.[20] The needle geometry of these crystals precluded all measurements other than those along the c-axis. In the case of $Pd(dpg)_2Br_{1.1}$, typical sample dimensions for the tetragonal needles were 0.50 to 1.0 mm in length and 0.01 to 0.05 mm in thickness, whereas for $Ni(dpg)_2Br_{1.0}$ the corresponding dimensions were 0.25 to 0.50 mm in length and ca. 0.0005 mm in thickness. Conductivity data were obtained using the conventional four-probe technique. Due to the small specimen size, considerable care was exercised in the electrode attachment and testing procedures. A special sample holder, which could simultaneously accommodate up to four crystals, was utilized. Each crystal was placed across four 0.025 mm diameter tungsten wires and joined with small droplets of Glydag. Following drying of the Glydag, each crystal was screened at room temperature for any non-ohmic or time-dependent behavior and replaced if necessary. The sample holder was then hermetically sealed and placed in the transport measurement apparatus. Bidirectional variable temperature runs were performed on a large number crystals with the low temperature limit determined by sample resistance greater than 10^{12} ohms. Keithley electrometers were utilized for the measurement of sample currents and voltages; a Keithley 225 current source was used to provide the sample current. The data were judged to be meaningful only when reproducible over several runs. The maximum error introduced

in conductivity measurements by the determination of sample cross-sectional area is estimated to be no greater than 10%.

No evidence for ionic conduction was observed; passing a steady 10 nA dc current through samples for two hours did not result in a continuous decline in conductivity which would be expected for carrier depletion by ionic drift. Approximate calculations indicate that complete polarization would occur in less than two hours for typical samples and currents as low as 10 nA.

RESULTS AND DISCUSSION

Chemistry

The reaction of $Pd(dpg)_2$ with bromine in hot o-dichlorobenzene is found to yield two crystalline products (eqs. (1) and (2)). In the case of relatively dilute solutions (see Experimental Section for details), lustrous red-brown needles

$$Pd(dpg)_2 + 0.55\ Br_2 \rightleftharpoons[o\text{-}C_6H_4Cl_2] Pd(dpg)_2Br_{1.1} \quad (1)$$

$$Pd(dpg)_2 + Br_2 \xrightarrow{o\text{-}C_6H_4Cl_2} Pd(dpg)_2Br_2 \cdot 2o\text{-}C_6H_4Cl_2 \quad (2)$$

of $Pd(dpg)_2Br_{1.1}$ are isolated. This material has previously been prepared by a somewhat different procedure;[4b] however, in our hands, only the present methodology consistently produces crystals of sufficient dimensions for single crystal, four-probe conductivity measurements. When the concentration of $Pd(dpg)_2$ is increased, brown parallelepipeds of the Pd(IV) complex, $Pd(dpg)_2Br_2 \cdot 2o\text{-}C_6H_4Cl_2$ (equation (2)), are also isolated. Using a procedure similar to the above palladium chemistry, red-brown needles of composition $Ni(dpg)_2Br_{1.0}$ can be prepared (eq. (3)). The

$$Ni(dpg)_2 + 0.50\ Br_2 \rightleftharpoons[o\text{-}C_6H_4Cl_2] Ni(dpg)_2Br_{1.0} \quad (3)$$

bromination of $Ni(dpg)_2$, using a somewhat different procedure,[4b] has been previously reported, yielding a maximum halogen: metal ratio similar to that observed in the present palladium bromide system. The $Ni(dpg)_2Br_{1.0}$ crystals could only be grown in a size marginally suitable for single crystal conductivity measurements. Attempts to grow crystals by slower cooling of the hot solutions (as was used for the $M(dpg)_2I$ materials)[4a] resulted in the complete decomposition of the $Ni(dpg)_2$. For $Pd(dpg)_2$, this procedure resulted in exclusive formation of $Pd(dpg)_2Br_2 \cdot 2o\text{-}C_6H_4Cl_2$. Attempts to grow crystals of either of the $M(dpg)_2Br_x$ materials by diffusion techniques were unsuccessful. For the present syntheses, the halogen:metal ratio in brominated $Pd(dpg)_2$ is greater than in the analogous iodinated material by

a factor of ca. 13 ± 8% . It will be seen that any greater content of bromine over iodine in $M(dpg)_2X$ compounds can be satisfactorialy explained by the smaller spacial demands of the polybromide species (Br_5^-) as compared to the analogous polyiodide (I_5^-) in lattice channels of essentially constant dimensionality (vide infra).

Resonance Raman Studies

In order to identify the form of bromine present in $Ni(dpg)_2Br_{1.0}$ and $Pd(dpg)_2Br_{1.1}$ and thus to measure the degree of partial oxidation, resonance Raman spectra-structure criteria analogous to those already employed in this Laboratory for polyiodides[3,4a,21-23] were developed. Such criteria must be based upon judiciously chosen model compounds of known structure. Figure 2 displays spectra of model compounds containing Br_2 (A), symmetrical ($D_{\infty h}$)Br_3^- (B), unsymmetrical Br_3^- (C), and symmetrical Br_5^- (D). Spectral data are compiled in Table I. As in the

$$Br - Br \qquad \underline{A}$$

$$[Br - Br - Br]^- \qquad \underline{B}$$

$$[Br - Br \cdots\cdot Br]^- \qquad \underline{C}$$

$$[Br - Br \cdots\cdot Br \cdots\cdot Br - Br]^- \qquad \underline{D}$$

case of polyiodides, the vibrational spectra of polybromides can be understood in terms of the interaction of Br_2 with species of various electron donating tendencies. Thus, in the formation of Br_3^-, Br_2 can be viewed as a Lewis acid which interacts with the Lewis base Br^-. Upon complexation of Br_2 with Br^-, Br-Br antibonding molecular orbitals are populated and the Br-Br bond is weakened; thus, the Br-Br distance is increased from 2.29(1)Å in Br_2[24] to 2.53(1)Å in $(C_6H_5)_4As^+Br_3^-$,[25] and the resulting force constant is lowered significantly from that in Br_2. In the Raman spectrum of Br_2 in benzene solution (Figure 2A), the fundamental stretching frequency is observed at 306cm^{-1}. The Raman spectrum of $(n\text{-}C_4H_9)_4N^+Br_3^-$, which has been shown by ^{81}Br nuclear quadrupole resonance[26] spectro-

scopy to contain symmetrical Br_3^- units (i.e., equal Br-Br distances), is shown in Figure 2B. The actual Br-Br stretching frequency in Br_3^- is given by the average of the symmetrically (166 cm^{-1}) and the antisymmetrically (191 cm^{-1})[27] coupled normal modes,[23] i.e., 179 cm^{-1}; hence, the stretching force constant (0.94 mdyn/Å)[28] has been lowered appreciably from that in Br_2(2.46 mdyn/Å).[28] In $CsBr_3$, the Br_3^- ions have been distorted by crystal forces, and Br-Br distances of 2.44(1)Å and 2.70(1)Å are observed.[29] Two Br-Br stretching modes at 208 cm^{-1} (further split by small solid state effects)[27] and 140 cm^{-1} are observed in the Raman spectrum of $CsBr_3$ (Figure 2C). Even greater distortion of the Br_3^- ion has been found in the unusual structure of PBr_4^+ Br_3^-, which exhibits grossly different tribromide ion Br-Br distances of 2.39(1) and 2.91(1)Å.[30] The Raman active Br-Br stretching modes for the Br_3^- ion in $PBr_4^+Br_3^-$ have been observed at 249 cm^{-1} and 135 cm^{-1}.[31] The Raman spectrum of the bromine analog of (trimesic acid·H_2O)$_{10}H^+I_5^-$ (which contains chains of linear I_5^- ions)[4a,32] is displayed in Figure 2D. This material is isomorphous with (trimesic acid·H_2O)$_{10}H^+I_5^-$, and the presence of Br_5^- ions is inferred.[33] It is significant to note that in all instances studied to date, polyiodides and polybromides of the same counterion have the same type of structure.[3a] The intense "Br_2" Br-Br scattering at 265 cm^{-1} in (trimesic acid·H_2O)$_{10}H^+Br_5^-$(analogous to the 160 cm^{-1} band in (trimesic acid·H_2O)$_{10}H^+I_5^-$ [4a]) can be explained in terms of the Lewis base Br^- distributing electron density between two Lewis acid Br_2 units; hence, to first order the Br-Br force constant in (trimesic acid·H_2O)$_{10}H^+Br_5^-$ is expected to be smaller than in Br_2 but larger than in ($\underline{n}$-C_4H_9)$_4N^+Br_3^-$. The weak scattering at 160 cm^{-1} may be attributed to a symmetric stretching mode which is predominantly $Br_2 \leftarrow Br \rightarrow Br_2$ in character. A similar band at 107 cm^{-1} was observed in the I_5^- system.[4a] Alternatively, this transition may be a Raman active π_g bending mode which is also predicted by the selection rules for $D_{\infty h}$ Br_5^-. The relative intensities of the bands in the Raman spectrum of (trimesic acid·H_2O)$_{10}H^+Br_5^-$ are insensitive to the laser excitation wavelength between 4579Å and 5145Å.

The solid state resonance Raman spectra of $Ni(dpg)_2Br_{1.0}$ and $Pd(dpg)_2Br_{1.4}$ are presented in Figure 3, and numerical data are tabulated in Table I. The spectra of $Ni(dpg)_2$ and $Pd(dpg)_2$ are displayed elsewhere.[4a] Intense Raman scattering at ca. 245 cm^{-1} and weaker scattering at ca. 157 cm^{-1} is observed in the spectra of both brominated complexes. The overtone and combination bands of these two transitions are also present at ca. 311 w(2 x 157), 402w (157 + 245), and 480 w (2 x 245)cm^{-1}. The $M(dpg)_2I$ materials display a transition near 157 cm^{-1} (at 160 cm^{-1}) which was assigned to a polyiodide vibration.[4a] That any coincidence or near coincidence with the present 157 cm^{-1} band is fortuitous (and not arising from the $M(dpg)_2^{\delta+}$ moiety) is further confirmed by the presence of the 157 + 245 combination band in the $M(dpg)_2Br_x$ materials. Clearly, the 157cm^{-1} scattering is associated with a polybromide species. In addition, the presence of the combination band assures that the structures giving rise to the 245 and 157 cm^{-1} bands are in close spacial proximity (i.e., they are not due to different compounds). In the $M(dpg)_2I$ materials, weak Raman transitions due to the $M(dpg)_2^{+0.2}$ units were assigned at 442 cm^{-1} (M=Ni) and at 448 cm^{-1} (M=Pd). It is interesting to note that these "markers" appear to be present at essentially the same energies in the brominated analogues discussed here.

As demonstrated in Figure 4, the relative intensities of the polybromide spectral features in the resonance Raman spectrum of $Ni(dpg)_2Br_{1.0}$ are not particularly sensitive to the laser excitation wavelength between 4579 and 5145Å. Attempts to obtain further vibrational information on the polybromide species in these materials by far-infrared spectroscopy have been unsuccessful due to the presence of intense $M(dpg)_2$ - centered modes in this region.

The resonance Raman data allow immediate rejection of Br_2 and symmetrical Br_3^- as major species present in $Ni(dpg)_2Br_{1.0}$ and $Pd(dpg)_2Br_{1.1}$. Although the results on $(trimesic\ acid \cdot H_2O)_{10}H^+Br_5^-$ argue strongly for the Br_5^- formulation, the similarity of chromophores in Br_5^-(D) and highly distorted Br_3^-(C) warrants further

discussion as to how, in general, such species may be differentiated. To begin with, the reasons for which symmetrical trihalide ions distort have been discussed at length.[34] Invariably the driving force for distortion is a spacially and electrostatically unsymmetrical environment; typically the trihalide is caused to distort by interaction with a proximate cation. In the $M(dpg)_2X$ structure (Figure 1) the halogen atoms are in an axially symmetric and nonpolar environment (the "tunnel" is lined with aromatic C-H residues). Thus, the driving force for severe Br_3^- distortion is not evident in the present case; the presence of such a species appears to be incompatible with the structural environment.

We now show that it is possible to predict the Br_5^- Raman spectrum from the corresponding I_5^- spectrum (or, indeed, the spectrum of any simple polybromide from that of the corresponding polyiodide), and that the result is in good agreement with the observed $M(dpg)_2Br$ spectrum. Stretching force constants in small molecules can be predicted with reasonable accuracy using the established empirical approach of Gordy[35] (eq.(4)). Here for diatomic oscillator AB, N is the bond order,

$$f = 1.67\ N \left(\frac{X_A X_B}{d^2} \right)^{3/4} + 0.30 \qquad (4)$$

d is the bond distance, and X_A and X_B are electronegativities of atoms A and B, respectively. To minimize the uncertainties in N and X and to take full advantage of the existing polyiodide data we propose the use of eq.(5), where the polybromide frequency can be related to frequencies calculated (cal) from eq.(4) and the experimental frequency of the analogous polyiodide (obs). Confidence in this approach is affirmed by the calculated parameters for Br_2 and Br_3^- in Table II, which are derived from equations (4) and (5), literature data for I_2 and I_3^-, and, in the case of X_3^-, the appropriate generalized valence force field equations[36] (estimating the

$$\nu_{Br} = (\nu_I)_{obs} (\nu_{Br})_{cal} / (\nu_I)_{cal} \qquad (5)$$

stretch-stretch interaction constant by an established method[28]). The results are in excellent agreement with experiment and, importantly, relatively insensitive to choice in N.[37] Thus, it should be possible to predict the Br_5^- vibrational spectrum beginning with I_5^- data and a reasonable estimate of the Br_5^- molecular structure.

The Br_5^- metrical parameters can be estimated by noting the near constancy of the following Br:I distance ratios[39]: covalent radii, 0.86;[39a] ionic radii, 0.83;[39b] halogen-halogen distance in the symmetrical trihalide, 0.87;[39c] and halogen-halogen distance in the distorted trihalide (with the same counterion), 0.86 and 0.89.[39d] The average of these Br:I distance ratios, 0.87 ± 0.01, multiplied by the known I_5^- distances,[4a,32] yields the pentabromide structure shown below (E). These metrical parameters for I_5^- and Br_5^- were next used in eq. (4) to calculate stretching

$$\underset{R}{Br\text{—}\overset{2.38\text{Å}}{}Br}\cdots\underset{r}{\overset{2.82\text{Å}}{}Br}\cdots\underset{r}{\overset{2.82\text{Å}}{}Br}\cdots\underset{R}{Br\text{—}\overset{2.38\text{Å}}{}Br} \qquad \underline{E}$$

force constants. Nearest neighbor stretch-stretch interaction constants (f_{Rr}, f_{rr}) in the secular equation for a linear pentaatomic molecule[40] were approximated as for the trihalides,[28] and non-nearest neighbor interaction constants (f_{RR}, f_{Rr_2}) were set equal to zero. It can be seen in Table III that the agreement between experimental Br_5^- frequencies and those predicted from eq. (5) using the (trimesic acid·H_2O)$_{10}H^+I_5^-$ Raman data[4a] is very good; agreement is also good when the $M(dpg)_2I$ spectral data are used as a starting point (Table III). The results are not particularly sensitive to reasonable choice of N, interaction constants, or bond distances.

A complementary way in which to assess the congruency between the polyiodide and polybromide vibrational data is by examining the ratio of the high to low energy Raman scattering transitions. As can be seen in Table IV, the pentahalide ratios fall within a relatively narrow range, distinct from all the other species tablulated. The distorted tribromides fall into two classes. The moderately asymmetric species (e.g., $CsBr_3$) have slightly smaller frequency ratios than Br_5^-, but the actual

frequencies are substantially lower. The latter effect no doubt arises from the greater concentration of negative charge on the single Br_3^- chromophore in tribromide (similar effects are evident in molecular orbital calculations,[38] ^{129}I Mössbauer isomer shifts,[4a] and nuclear quadrupole coupling constants[4a,41]). The result of the more localized negative charge is a greater reduction in bond orders and force constants than in the pentahalide (lower electronegativities in terms of eq.(4)). The second class of distorted tribromides, those evidencing extreme distortion, is represented by $PBr_4^+Br_3^-$; here the high frequency stretch approaches that of Br_5^- (becomes more "Br_2 - like"). However, the low energy stretching mode of this Br_3^- ion is considerably below that of Br_5^- . Again the more concentrated negative charge explains this effect. A large, positive stretch-stretch interaction constant, $f_{rr}(E)$, would further raise the energy of the low frequency mode in Br_5^- .

To summarize, the form of bromine in the $M(dpg)_2Br$ materials, as deduced from our resonance Raman data employing several lines of argument, can be assigned predominantly, if not exclusively, to Br_5^-. Thus, we estimate the charges on the metal-ligand units as $Ni(dpg)_2^{+0.2(2)}$ and $Pd(dpg)_2^{+0.2(2)}$.

Electronic Absorption Spectra

The electronic absorption spectra of the $M(dpg)_2$ and $M(dpg)_2Br_x$ systems, M=Ni, Pd, are presented in Figure 5A-D, and the data are compiled in Table V. Upon bromination the lowest energy bands at 515 nm in $Ni(dpg)_2$ and 445 nm in $Pd(dpg)_2$ are shifted to lower energies, 520 nm and 455 nm, respectively. This is consistent with the assignment of these features to intramolecular $nd_{z^2} \rightarrow (n+1)p_z$ transitions which borrow intensity from intermolecular metal-metal charge transfer transitions.[42] The energies of such solid state electronic transitions in stacked d^8 palladium and nickel bisglyoximates have been demonstrated to be polarized parallel to the chain direction[42] and to be sensitive to intrastack metal-metal separation.[42,43] Thus,

upon bromination of the $M(dpg)_2$ materials, the intrastack metal-metal distances are decreased (by 0.20Å for M=Ni;[4,16] by 0.24Å for M=Pd[4,16]) and, as anticipated, the low energy bands are red-shifted. The bands in $M(dpg)_2$ at 435 nm(M=Ni) and 365 nm (M=Pd) can be assigned[42] to intramolecular metal-ligand $(d\pi \rightarrow \pi)^*$ transitions and are expected to be rather insensitive to metal-metal separation.[42] In support of metal-ligand origin, the bands are present at essentially the same energy in the $M(dpg)_2I$[4a] and $M(dpg)_2Br_x$ materials. An intense, broad, underlying feature is also observed at lower energies (400-550 nm) in the spectra of the $M(dpg)_2Br_x$ materials. A similar, broad absorption centered at 425 nm is evident in the spectrum (Figure 5E) of the Br_5^- chain compound (trimesic acid·$H_2O)_{10}H^+Br_5^-$. Transitions in the region 400-475 nm have also been observed in the solid state electronic spectra of Br_3^- compounds.[44] Therefore, it is not unreasonable to assign the broad feature in the spectra of the $M(dpg)_2Br_x$ materials to transitions within the polybromide chains, as argued for the corresponding polyiodide systems.[4a] It is these transitions which are doubtless responsible for the resonant enhancement of the polybromide Raman spectra.

Electrical Conductivity

Single crystal measurements of $Ni(dpg)_2Br_{1.0}$ and $Pd(dpg)_2Br_{1.4}$ conductivity were performed as a function of temperature by the four-probe technique. The thinness of the crystals only permitted transport measurements in the needle direction. Because comparison of $M(dpg)_2Br_x$ and $M(dpg)_2I$ conductivities was a major goal in this investigation, great care was taken to insure that specimens and contacts were of the highest possible quality

In Figures 6 and 7 are shown representative variable temperature conductivity data comparing the iodinated and brominated complexes of nickel (Figure 6) and palladium (Figure 7). The data adhere closely to a linear $\ln \sigma$ vs. $1/T$ relationship over the temperature range investigated. As in the case of the

$M(dpg)_2I$ materials,[4a] the data could be fit by the method of least-squares to a thermal activation model (eq.(6)) with the parameters compiled in Table VI.

$$\sigma = \sigma_o e^{-\Delta/kT} \quad (6)$$

Several features are obvious upon viewing the conductivity data. First, as in the case of iodine doping,[4a] bromination has brought about a very large increase (ca. 10^7-10^8) in the metal bisdiphenylglyoximate charge transport capacity. Secondly, there is no clear-cut evidence that bromination produces materials with significantly and uniformly different charge transport characteristics than iodination. Thus, although the brominated derivative is perhaps slightly more conductive and has a lower activation energy for conduction in the palladium system, the exactly opposite trend is observed in the nickel system. These results argue against the halogen chains being the principal conduction pathway. As was noted earlier, the iodine-containing chains would be expected, all other factors being equal, to be far more efficient charge carriers than the bromine-containing chains.[18] This expectation is not confirmed by the conductivity data. Indeed, for the nickel and palladium bisdiphenylglyoximates, the effect of changing the halogen is no greater than changing the metal (which is a relatively small effect in this and most other partially oxidized metallomacrocycle systems).[3-8] It is interesting to note that the nickel complex is somewhat more conductive than the palladium analogue which was also found for the $M(dpg)_2I$ systems.[4a] Additional evidence for the major conduction pathway being the $M(dpg)_2^{\delta+}$ stacks is derived from thermoelectric power measurements. These will be discussed in detail elsewhere.[45] We note here that for $Ni(dpg)_2I$, $S = +40\ \mu V/^\circ K$, and that for $Pd(dpg)_2Br$, $S = +127\ \mu V/^\circ K$. The positive sign can be taken as evidence for hole conduction,[8b,10a,b,46] and the similarities in the iodide/bromide data again underscore the close congruencies in transport characteristics for the materials with different halogens.

CONCLUSIONS

Bromination of $Ni(dpg)_2$ and $Pd(dpg)_2$ yields the partially oxidized materials $Ni(dpg)_2Br_{1.0}$ and $Pd(dpg)_2Br_{1.1}$, in which the predominant, if not exclusive, halogen-containing species is Br_5^-. Resonance Raman spectroscopy represents a powerful tool for the structural identification of polybromides, and simple empirical relationships permit the prediction of polybromide spectra from those of the analogous polyiodides. The degree of $M(dpg)_2$ partial oxidation in the present case (ca.+0.20(2), M=Ni; ca. +0.22(2), M=Pd) is equal to or only slightly greater than that in the iodine-doped analogues (+0.20) (a similar observation was made in the case of tetrathiafulvalenium iodides and bromides[9e]). Any differences in $M(dpg)_2X$ oxidation states arise from a slightly greater degree of bromine incorporation. In this regard, it is interesting to note that the 0.87 bromine to iodine size relationship mentioned earlier leads to a maximum possible predominance of bromine over iodine of ca.1.15 in the filling of isostructural lattice tunnels.The transport properties of the $M(dpg)_2Br$ compounds do not differ greatly from those of the $M(dpg)_2I$ compounds, and it therefore seems unreasonable that the halogen chains provide the dominant pathway for charge conduction.

ACKNOWLEDGEMENTS

This research was generously supported by the Office of Naval Research (to T.J.M.) and by the NSF-MRL program through the Materials Research Center of Northwestern University (grants DMR76-80847A01 and DMR79-23573).

REFERENCES

1. a. Department of Chemistry and the Materials Research Center.

   b. Department of Electrical Engineering and Computer Science, and the Materials Research Center.

   c. Camille and Henry Dreyfus Teacher-Scholar.

2. a. Devreese, J.T.; Evrard, V.E.; Van Doren, V.E., eds., Highly Conducting One-Dimensional Solids, Plenum Press, N.Y., 1979.

   b. Torrance, J.B. Accts. Chem. Res, 1979, 12, 79-86.

   c. Miller, J.S.; Epstein, A.J., eds., Synthesis and Properties of Low-Diemnsional Materials, Ann. N.Y. Acad. Sci., 1978, 313.

   d. Keller, H.J., ed. Chemistry and Physics of One-Dimensional Metals, Plenum Press, New York, 1977.

   e. Miller, J.S.; Epstein, A. J. Prog. Inorg. Chem., 1976, 20, 1 - 151.

   f. Keller, H.J., ed. Low Dimensional Cooperative Phenomena, Plenum Press, N.Y. 1975.

   g. Soos, Z.G.; Klein, D.J. in Molecular Associations, Foster, R., ed., Academic Press, N.Y. 1975, Chapt. 1.

3. a. Marks, T.J.; Kalina, D.W. in "Extended Linear Chain Compounds," Miller, J.S. ed., Plenum Publishing Corp., in press.

   b. Marks, T.J. Ann. N.Y. Acad. Sci., 1978, 313, 594-616.

4. a. Cowie, M.A.; Gleizes, A.; Grynkewich, G.W.; Kalina, D.W.; McClure, M.S.; Scaringe, R.P.; Teitelbaum, R.C.; Ruby, S.L.; Ibers, J.A.; Kannewurf, C.R.; Marks, T.J. J. Am. Chem. Soc., 1979, 101, 2921-2936, and references therein.

   b. Miller, J.S.; Griffiths, C.H. J. Am. Chem. Soc., 1977, 99, 749-755.

   c. Gleizes, A.; Marks, T.J.; Ibers, J.A. J. Am. Chem. Soc., 1975, 97, 3545-3546.

5. a. Petersen, J.L.; Schramm, C.S.; Stojakovic, D.R.; Hoffman, B.M.; Marks, T.J. J. Am. Chem. Soc., 1977, 99, 286-288.

   b. Schramm, C.S.; Stojakovic, D.R.; Hoffman, B.M.; Marks, T.J. Science, 1978, 200, 47-48.

   c. Scaringe, R.P.; Schramm, C.J.; Stojakovic, D.R.; Hoffman, B.M.; Ibers, J.A.; Marks, T.J, J. Am. Chem. Soc., in press.

   d. Schoch, K.F., Jr.; Kundalkar, B.R.; Marks, T.J. J. Am. Chem. Soc., 1979, 101, 7071-7073.

e. Marks, T.J.; Schoch, K.F., Jr.; Kundalkar, B.R. Synth. Met., 1980, 1, 337-347.

f. Dirk, C.W.; Lyding, J.W.; Schoch, K.F., Jr.; Kannewurf, C.R.; Marks, T.J. Polymer Preprints, in press.

6. a. Lin, L.-S.; McClure, M.S.; Lyding, J.W.; Ratajack, M.T.; Wang, T.-C.; Kannewurf, C.R.; Marks, T.J., J. Chem. Soc., Chem. Comm., in press.

b. McClure, M.S.; Lin, L.-S.; Whang, T.-C.; Ratajack, M.T.; Kannewurf, C.R.; Marks, T.J. Bull. Am. Phys. Soc., 1980, 25,315.

7. a. Brown, L.D.; Kalina, D.W.; McClure, M.S.; Ruby, S.L.; Schultz, S.; Ibers, J.A.; Kannewurf, C.R.; Marks, T.J. J. Am. Chem. Soc., 1979, 101, 2937-2946.

b. Marks, T.J.; Webster, D.F.; Ruby, S.L.; Schultz, S. J. Chem. Soc. Chem. Commun., 1976, 444-445.

c. Endres, H.; Keller, H.J.; Megnamisi-Bélombé, M.; Moroni,W.;Nöthe,D. Inorg. Nucl. Chem. Lett., 1974, 10, 467-471.

d. Endres, H.; Keller, H.J.; Moroni, W.; Weiss, J. Acta Cryst., 1975, B31, 2357-2358.

e. Endres, H.; Keller, H.J.; Megnamisi-Bélombé, M.; Moroni, W.; Pritzkow, H.; Weiss, J.; Comes R. Acta Cryst., 1976, A32, 954-957.

8. Wright, S.K.; Schramm, C.J.; Phillips, T.E.; Scholler, D.M.; Hoffman, B.M. Synth. Met., 1979, 1, 43-51.

9. a. Teitelbaum, R.C.; Johnson, C.K.; Marks, T.J. J. Am. Chem. Soc., 1980, 102, 2986-2989, and references therein.

b. Somoano, R.B.; Gupta, A.; Hadek, V.; Datta, T.; Jones, M.; Deck, R.; Hermann, A.M. J. Chem. Phys., 1975, 63, 4970-4976.

c. Warmack, R.J.; Callcott, T.A.; Watson, C.R. Phys. Rev. B, 1975, 12, 3336-3338.

d. Scott, B.A.; LaPlaca, S.J.; Torrance, J.B.; Silverman, B.D.; Welber, B. J. Amer. Chem. Soc., 1977, 99, 6631-6639, and references therein.

e. Johnson, C.K.; Watson, C.R. Jr.; Warmack, R.J. Abstracts, 25th Meeting of the American Crystallographic Association, 1975, SC6, p. 19.

f. Johnson, C.K.; Watson, C.R., Jr.; Warmack, R.J. Ann. Prog. Report. Chem. Div., Oak Ridge National Laboratory, Oak Ridge, Tenn., 1976, p. 102-103.

10. a. Khanna, S.K.; Yen, S.P.S.; Somoano, R.B.; Chaikin, P.M.; Ma, C.L.; Williams,R.; Samson, S. Phys. Rev. B, 1979, 19, 655-663, and references therein.

b. Isett, L.C. Phys. Rev. B, 1978, 18, 439-447, and references therein.

c. Smith, D.L.; Luss, H.R. Acta Cryst., 1977, B33, 1744-1749.

d. Buravov, L.I.; Zvereva, G.I.; Kaminskii, V.F.; Rosenberg, L.P.; Khidekel, M.L.; Shibaeva, R.P.; Shchegolev, I.F.; Yagubskii, E.B. J. Chem. Soc. Chem. Commun., 1976, 720-721.

11. a. Kámaras, K.; Mihály, G.; Grüner, G.; Jánossy, A. J. Chem. Soc. Chem. Commun., 1978, 974-975.

b. Kamaras, K.; Kertesz, M. Solid State Commun., 1978, 28, 607-611.

12. a. Teitelbaum, R.C.; Ruby, S.L.; Marks, T.J. J. Am. Chem. Soc., 1980, 102, 3322-3328, and references therein.

b. Teitelbaum, R.C.; Ruby, S.L.; Marks, T.J. J. Am. Chem. Soc., 1979, 101, 7568-7573.

13. Perlstein, J.H. Angew. Chem. Int. Ed. Engl., 1977, 16, 519-534.

14. a. Huml, K. Acta Cryst., 1967, 22, 29-32.

b. Hadek, V. J. Chem. Phys., 1968, 49, 5202-5203.

15. Underhill, A.E.; Watkins, D.M.; Pethig, R. Inorg. Nucl. Chem. Lett., 1973, 9, 1269-1273.

16. Foust, A.S.; Soderberg, R.H. J. Am. Chem. Soc., 1967, 89, 5507-5508.

17. $Ni(dpg)_2Br$: a = 19.51(6), c = 6.72(2)Å;[16] $Ni(dpg)_2I$: a = 19.887(4), c = 6.542(2)Å;[4a] $Pd(dpg)_2Br$: a = 19.78(6), c = 6.57(2)Å;[16] $Pd(dpg)_2I$: a = 20.17(6), c = 6.52(2)Å.[16]

18. Assuming stoichiometry, crystal structure, and form of polyhalide remain essentially constant in analogous brominated and iodinated materials, then differences in conductivity are expected to arise from the non-equivalent polarizabilities, ionization potentials, electron affinities, and sizes of I and Br, which would lead to vastly different electron correlation and transfer integrals for I and Br in, for example, the one-dimensional Hubbard description.[2] As an illustration, elemental iodine becomes metallic under moderate pressure, whereas elemental bromine does not:

a. Riggleman, B.M.; Drickamer, H.G. J. Chem. Phys., 1963, 38, 2721-2724.

b. Chao, M.S.; Stenger, V.A. Talanta, 1964, 11, 271-281, and references therein.

19. a. Wells, H.L. Z. Anorg. Chem., 1892, 1, 85-97.

b. Popov, A. I.; Buckles, R.E. Inorg. Syn., 1957, 5, 167-175.

20. Lyding, J.W.; Kannewurf, C.R. manuscript in preparation.

21. Teitelbaum, R.C.; Ruby, S.L.; Marks, T.J. J. Am. Chem. Soc., 1978 100, 3215-3217.

22. Teitelbaum, R.C.; Ruby, S.L.; Marks, T.J. J. Am. Chem. Soc., in press.

23. Kalina, D.W.; Stojakovic, D.R.; Teitelbaum, R.C.; Marks, T.J. manuscript in preparation.

24. Handbook of Chemistry and Physics, 57th ed., Chemical Rubber Publishing Co., Cleveland, Ohio 1976-1977, p. F-216.

25. Ollis, J.; James, V.J.; Ollis, D.; Bogaard, M.P. Cryst. Struct. Commun., 1976, 5, 39-42.

26. Kume, Y.; Nakamura, D. J. Magn. Reson., 1976, 21, 235-240.

27. Gabes, W.; Gerding, H. J. Mol. Struct., 1972, 14, 267-279.

28. Gabes, W.; Elst, R. J. Mol. Struct., 1974, 21, 1-5.

29. Breneman, G.L.; Willett, R.D. Acta Cryst., 1969, B25, 1073-1076.

30. Breneman, G.L.; Willett, R.D. Acta Cryst., 1967, 23, 467-471.

31. a. Gabes, W.; Gerding, H. Rec. Trav. Chim., 1971, 90, 157-164.

b. The band at 249 cm^{-1} is split to 247 and 251 cm^{-1} by small solid state effects.[31a]

32. Herbstein, F.H.; Kapon, M. Acta Cryst., 1972, A28, S74, and private communication.

33. Herbstein, F.H.; Kapon, M.; Reisner, G. M.; Proc. Royal Soc., in Press.

34. a. Rundle, R.E. Acta Cryst., 1961, 14, 585-589.

b. Brown, R.D.; Nunn, E.K. Austral. J. Chem., 1966, 19, 1567-1576.

c. Migchelsen, T.; Vos, A. Acta Cryst., 1967, 22, 812-815.

35. a. Kugimiya, K.; Steinfink, H. Inorg. Chem., 1968, 7, 1762-1770.

b. Wells, A.F. Structural Inorganic Chemistry, 3rd Edition, Oxford University Press, London, 1962, p. 64.

c. Gordy, W. J. Chem. Phys., 1946, 14, 305-320.

36. a. For symmetric X_3^-, the generalized valence force field equations are $\nu_1 = \frac{1}{2\pi}[(f_1 + f_{11})/m_x]^{1/2}$ and $\nu_3 = \frac{1}{2\pi}[3(f_1 - f_{11})/m_x]^{1/2}$; see Herzberg, G.N. Infrared and Raman Spectra of Polyatomic Molecules, D. van Nostrand Co., Inc., New York, 1945, p. 153-154

b. For unsymmetrical X_3^-, the generalized valence force field equations are $\lambda_1 + \lambda_3 = 4\pi^2(\nu_1^2 + \nu_3^2) = \frac{2}{m}(f_1 + f_2 - f_{12})$ and $\lambda_1\lambda_3 = 16\pi^4\nu_1^2\nu_3^2 = \frac{3}{m_x^2}(f_1f_2 - f_{12}^2)$; see Richardson, W.S.; Wilson, E.B., Jr. J. Chem. Phys., 1950, 18, 694-696.

37. Previous bond order determinations, based upon experimental spectroscopic data[28] and upon molecular orbital calculations,[38] indicate that N = 1 for X_2[28,35c] and N = 0.38[28] - 0.71[38] for X_3^- are reasonable values.

38. a. Datta, S.N.; Ewig, C.S.; Van Wazer, J. R. J. Mol. Struct., 1978, 48, 407-416.

b. Gabes, W.; Nijman-Meester, M.A.M. Inorg. Chem., 1973, 12, 589-592.

c. Wiebenga, E.H.; Kracht, D. ibid., 1969, 8, 738-746.

39. a. Cotton, F.A.; Wilkinson, G. Advanced Inorganic Chemistry, John Wiley and Sons, New York, p. 117.

b. Shannon, R.D. Acta Cryst., 1976, A32, 751-767.

c. ref. 25, and Runsink, J.; Swen-Walstra, S.; Migchelson, T. Acta Cryst., 1972, B28, 1331-1335.

d. ref. 29, and Runsink, J.; Swen-Walstra, S.; Migchelson, T. Acta Cryst., 1972, B28, 1331-1335.

40. For symmetric X_5^-, the generalized valence force field equation for the Raman-active stretching frequencies is $\lambda^2 - \lambda[\frac{1}{m_x}(2f_R + f_{RR} + f_r + f_{rr} - 2f_{Rr_1} - 2f_{Rr_2})] + \frac{1}{m_x^2}[(f_R - f_{RR})(f_r + f_{rr}) - (f_{Rr_1} + f_{Rr_2})^2] = 0$, where $\lambda_+ = 4\pi^2\nu_1^2$ and $\lambda_- =$

$4\pi^2\nu_{\frac{1}{2}}^2$; see Smith, W.H.; Leroi, G.E. J. Chem. Phys., 1966, 45, 1767-1777, and Long, D.A.; Murfin, F.S.; Williams, R.L. Proc. Royal Soc., 1954, A223, 251-266.

41. a. Breneman, G.L.; Willett, R.D. J. Phys. Chem., 1967, 71, 3684-3686.

    b. Lucken, E.A.C. Nuclear Quadrupole Coupling Constants, Academic Press, New York, 1969, Chapt. 12.

42. a. Anex, B.G. A.C.S. Symposium Series, 1974, 5, 276-300.

    b. Hara, Y.; Shirotani, I.; Onodera, A. Solid State Commun., 1976, 19, 171-175.

    c. Ohashi, Y.; Hanazaki, I.; Nagakura, S. Inorg. Chem., 1970, 9, 2551-2556.

    d. Nishida, Y.; Kozuka, M.; Nakamoto, K. Inorg. Chim. Acta, 1979, 34, L273-L275.

43. a. Anex, B.G.; Krist, F.K. J. Am. Chem. Soc., 1967, 89, 6114-6125.

    b. Banks, C.V.; Barnum D.W. J. Am. Chem. Soc., 1958, 80, 4767-4772.

    c. Basu, G.; Cook, G.M.; Belford, R.L. Inorg. Chem., 1964, 3, 1361-1368.

    d. Zahner, J.C.; Drickamer, H.G. J. Chem. Phys., 1960, 33, 1625-1628.

44. Gabes, W.; Stufkens, D.J. Spectrochim. Acta, 1974, A30, 1835-1841.

45. Lyding, J.W.; Kannewurf, C.R.; Marks, T.J., manuscript in preparation.

46. Chaikin, P.M.; Grüner, G.; Shchegolev, I.F.; Yagubskii, E.B. Solid State Comm., 1979, 32, 1211-1214.

TABLE I

Resonance Raman Vibrational Data[a] for $M(dpg)_2$ and $M(dpg)_2Br_x$, M=Ni, Pd, and Model Polybromide Systems

Compound	$\bar{\nu}$ (cm^{-1})[b]
$Ni(dpg)_2$	418 ms, 113 w(br), 91 vw, 71 vw
$Ni(dpg)_2Br_{1.0}$	485 mw(br), 442 vw, 405 vw, 312 vw(br), 247 vs, 158 w
$Pd(dpg)_2$	405 vw, 166 vw, 133 vw, 82 w(sh), 69 vw
$Pd(dpg)_2Br_{1.1}$	475 mw(br), 448 vw, 400 vw, 310 vw(br), 244 vs, 156 w
(Trimesic acid · $H_2O)_{10}H^+Br_5^-$	265s, 160w
Br_2 in benzene	306s
$(n\text{-}C_4H_9)_4N^+Br_3^-$	301 vw, 264 vw, 251 vw, 191 w, 166s, 73 w
$Cs^+Br_3^-$	342 w(br), 232 m(sh), 215 s, 201 s, 140 m, 125 w, 120 w, 105 w, 78 m, 66 m
$PBr_4^+ Br_3^-$ [c]	251 s, 247 s, 135 m, 94 m

[a] Polycrystalline samples; Ar^+ 5145 Å excitation; range recorded: 50-500 cm^{-1}.

[b] Key: s=strong, m=medium, w=weak, v=very, sh-shoulder.

[c] Data taken from reference 31a for Br_3^- moiety only.

TABLE II

Calculated Vibrational Stretching Frequencies for Br_2, Symmetric Br_3^-, and Asymmetric Br_3^-, Using Equations (4) and (5) [a]

X_2 [b,c]

$(\nu_I)_{obs}$ (cm^{-1}) [d]	$(\nu_{Br})_{obs}$ (cm^{-1})	N in Eq. 4	$\nu_{Br} = (\nu_I)_{obs} \frac{(\nu_{Br})_{cal}}{(\nu_I)_{cal}}$ (cm^{-1})
209 [e]	306 [f]	1	316
		0.5	310

Symmetric (X_3^-) [g,h]

$(\nu_I)_{obs}$ (cm^{-1})	$(\nu_{Br})_{obs}$ (cm^{-1})	N in Eq. 4	$f_{11}(I)$ [i]	$f_{11}(Br)$ [i]	$\nu_{Br} = (\nu_I)_{obs} \frac{(\nu_{Br})_{cal}}{(\nu_I)_{cal}}$ (cm^{-1})
118, 145 [e,j]	166, 191 [f,j]	1	$0.36f_1$	$0.42f_1$	178, 205
		0.5	$0.36f_1$	$0.42f_1$	175, 200
		0.4	$0.36f_1$	$0.42f_1$	173, 199
		0.3	$0.36f_1$	$0.42f_1$	170, 196

Asymmetric (X_3^-) [k,l]

$(\nu_I)_{obs}$ (cm^{-1})	$(\nu_{Br})_{obs}$ (cm^{-1})	N_1, N_2 in Eq. 4	$f_{12}(I)$ [i]	$f_{12}(Br)$ [i]	$\nu_{Br} = (\nu_I)_{obs} \frac{(\nu_{Br})_{cal}}{(\nu_I)_{cal}}$ (cm^{-1})
99, 146 [e,j]	140, 208 [f,j]	0.5, 0.5	0.25	0.34	142, 210
		0.5, 0.2	0.25	0.34	138, 207
		0.4, 0.2	0.25	0.34	138, 205

Table II (continued)

[a] In equation (4), the electronegativities, χ, used to calculate force constants were 2.5 for I and 2.8 for Br; see ref. 39a, p. 115.

[b] Bond lengths, d, for equation (4) were obtained from ref. 24.

[c] Frequencies $(\nu)_{cal}$ were calculated from $\lambda = 4\pi^2\nu^2 = \frac{f}{\mu}$, where μ is the reduced mass.

[d] All frequencies given are in cm^{-1}.

[e] Ref 4a.

[f] This work.

[g] Bond lengths were obtained from refs. 25 and 39c.

[h] Frequencies $(\nu)_{cal}$ were calculated from the general valence force field equations given in ref. 36a.

[i] Interaction constants were taken from ref. 28; units are mdyn/Å.

[j] Ref. 27.

[k] Bond lengths were obtained from refs. 29 and 39c.

[l] Frequencies $(\nu)_{cal}$ were calculated from the general valence force field equations given in ref. 36b.

TABLE III

Calculated Raman-Active Vibrational Stretching Frequencies for $D_{\infty h}$ Br_5^- Using Equations (4) and (5) [a,b]

$(\nu_{I_5^-})_{obs}(cm^{-1})$[c]	$(\nu_{Br_5^-})_{obs}(cm^{-1})$[d]	N_R, N_r in Eq. 4	d_R, d_r (Å) in Br_5^-	f_{rr}[e] I	f_{rr}[e] Br	f_{Rr}[f] (mdyn/Å) I	f_{Rr}[f] (mdyn/Å) Br	$\nu_{Br_5^-}=(\nu_{I_5^-})_{obs}(\nu_{Br_5^-})_{cal}/(\nu_{I_5^-})_{cal}(cm^{-1})$[g]
104[h],162[i]	157,245	1,0.5	2.38,2.82	$0.36f_r$	$0.42f_r$	0.25	0.34	154,240
		1,0.5	2.38,2.82	$0.36f_r$	$0.42f_r$	0.15	0.20	147,240
		1,0.5	2.38,2.82	$0.36f_r$	$0.42f_r$	0.35	0.47	154,240
		1,0.5	2.38,2.82	$0.50f_r$	$0.58f_r$	0.25	0.34	155,240
		1,0.5	2.38,2.82	$0.50f_r$	$0.58f_r$	0.35	0.47	155,241
		0.7,0.3	2.38,2.82	$0.36f_r$	$0.42f_r$	0.25	0.34	151,237
		1,0.5	2.37,2.83	$0.36f_r$	$0.42f_r$	0.25	0.34	154,241
		1,0.5	2.36,2.84	$0.36f_r$	$0.42f_r$	0.25	0.34	154,241
		1,0.5	2.35,2.85	$0.36f_r$	$0.42f_r$	0.25	0.34	154,242
		1,0.5	2.34,2.86	$0.36f_r$	$0.42f_r$	0.25	0.34	153,242
		1,0.5	2.33,2.87	$0.36f_r$	$0.42f_r$	0.25	0.34	153,243
		1,0.5	2.28,2.92	$0.36f_r$	$0.42f_r$	0.25	0.34	151,246
		1,0.5	2.39,2.81	$0.36f_r$	$0.42f_r$	0.25	0.34	153,240
		1,0.5	2.40,2.80	$0.36f_r$	$0.42f_r$	0.25	0.34	153,239
		1,0.5	2.41,2.79	$0.36f_r$	$0.42f_r$	0.25	0.34	153,238
		1,0.5	2.42,2.78	$0.36f_r$	$0.42f_r$	0.25	0.34	154,238
		1,0.5	2.43,2.77	$0.36f_r$	$0.42f_r$	0.25	0.34	155,238
		1,0.5	2.48,2.72	$0.36f_r$	$0.42f_r$	0.25	0.34	155,235

Table III (continued)

[a] In equation (4), the electronegativities, χ, used to calculate force constants were 2.5 for I and 2.8 for Br; see ref. 39a, p. 115.

[b] Br-Br bond lengths used in equation (4) to calculate force constants for the Br_5^- ion were obtained by multiplying the I-I bond lengths in (trimesic acid·H_2O)$_{10}H^+I_5^-$ (refs. 32 and 4a) by 0.87 (see text).

[c] Raman data for (trimesic acid·H_2O)$_{10}H^+I_5^-$ were taken from ref. 4a; all frequencies given are in cm^{-1}.

[d] Raman data for M(dpg)$_2$Br$_x$ materials, M=Ni, Pd; see Table I. These values represent the averages of the Raman data for M=Ni and M=Pd.

[e] Interaction constants were taken from ref. 28 and then were allowed to vary. Typical results are given.

[f] Interaction constants were taken from ref. 28 and then were allowed to vary. Typical results are given.

[g] Frequencies $(\nu)_{cal}$ were calculated from the general valence force field equation given in ref. 40 (see text).

[h] In M(dpg)$_2$I, this band is observed at 107 (M=Ni) and 104 (M-Pd) cm^{-1} (ref. 4a).

[i] In M(dpg)$_2$I, this band is observed at 162 (M=Ni) and 160 (M=Pd) cm^{-1} (ref. 4a).

TABLE IV

Ratios of the High to Low Energy Vibrational Stretching Transitions[a] in Polyhalides

Species	X	$(\nu)_{High}$ (cm^{-1})	$(\nu)_{Low}$ (cm^{-1})	$(\nu)_{High}/(\nu)_{Low}$
symm. X_3^-	I	145[b]	118[b]	1.23
	Br	191[c]	166[c]	1.15
asymm. X_3^-	I	146[b]	99[b]	1.47
	Br	208[c]	140[c]	1.48
X_5^-	I	162[d]	104[d]	1.56
		162[e]	107[e]	1.51
		160[f]	104[f]	1.54
	Br	247[g]	158[g]	1.56
		244[h]	156[h]	1.56
		265[i]	160[i]	1.65
Extremely distorted X_3^-	Br	249[j]	135[j]	1.84

[a] Stretching frequencies given are in cm^{-1}.

[b] Refs. 4a and 27.

[c] Refs. 27 and this work.

[d] Ref. 4a; data for (trimesic acid·H_2O)$_{10}H^+I_5^-$.

[e] Ref. 4a; data for $Ni(dpg)_2I$.

[f] Ref. 4a; data for $Pd(dpg)_2I$.

[g] This work; data for $Ni(dpg)_2Br_{1.0}$.

[h] This work; data for $Pd(dpg)_2Br_{1.1}$.

[i] This work; data for (trimesic acid·H_2O)$_{10}H^+Br_5^-$.

[j] Ref. 31.

TABLE V

Electronic Spectral Data[a] for $M(dpg)_2$ and $M(dpg)_2Br_x$, M=Ni, Pd, as Nujol Mulls

Compound	Absorption, nm ($x10^3 cm^{-1}$)	
$Ni(dpg)_2$	285	(35.1)
	335 sh	(29.9)
	372 sh	(26.9)
	435	(23.0)
	515	(19.4)
$Ni(dpg)_2Br_{1.0}$	285	(35.1)
	335 sh	(29.9)
	375 sh	(26.7)
	440	(22.7)
	485	(20.6)
	520	(19.2)
	570 sh	(17.5)
	650 sh	(15.4)
$Pd(dpg)_2$	235	(42.6)
	278	(36.0)
	365	(27.4)
	445	(22.5)
$Pd(dpg)_2Br_{1.1}$	235	(42.6)
	280	(35.7)
	360	(27.8)
	455	(22.0)
	500	(20.0)
	600 sh	(16.7)

[a] Range recorded: 200-2100 nm; sh=shoulder.

TABLE VI

Single Crystal Four-Probe Electrical Conductivity Data for Partially Oxidized Metal Bisdiphenylglyoximates.

Material	dc Conductivity[a] at 295° K $(\Omega\text{-cm})^{-1} \times 10^4$	Δ(eV)[b]	$c/2$(Å)[c]
$Pd(dpg)_2Br_{1.1}$	0.8-1.5	0.208 ± 0.002	3.28(1)
$Pd(dpg)_2I$	0.2-0.8	0.388 ± 0.002	3.26(1)
$Ni(dpg)_2Br_{1.0}$	3.8-9.1	0.327 ± 0.002	3.36(1)
$Ni(dpg)_2I$	18-55	0.184 ± 0.0008	3.271(2)
$Pd(dpg)_2$[d]	$< 8 \times 10^{-5}$		
$Ni(dpg)_2$[d]	$< 8 \times 10^{-5}$		

[a] Range given for specimens examined.

[b] From least-squares fit to equation (6).

[c] Interplanar separation; see ref. 17.

[d] From ref. 4a.

Figure Captions

Figure 1. A stereo view of the unit cell of $Ni(dpg)_2I$ taken from reference 4a. The a axis is horizontal to the right, the b axis is vertical from bottom to top, and the c axis is toward the reader. The vibrational ellipsoids are drawn at the 50% level, except hydrogen atoms which are drawn arbitrarily small.

Figure 2. Resonance Raman spectra (5145 Å excitation) of A. Br_2 dissolved in benzene, B. Polycrystalline $(n\text{-}C_4H_9)_4N^+Br_3^-$, C. Polycrystalline $Cs^+Br_3^-$, D. Polycrystalline (trimesic acid$\cdot H_2O)_{10}H^+Br_5^-$.

Figure 3. Resonance Raman spectra (5145 Å excitation, polycrystalline samples) of $Pd(dpg)_2Br_{1.1}$ and $Ni(dpg)_2Br_{1.0}$.

Figure 4. Raman spectra of $Ni(dpg)_2Br_{1.0}$ (polycrystalline sample) with A. 4579 Å excitation, B. 4880 Å excitation, C. 5145 Å excitation.

Figure 5. Electronic absorption spectra (polycrystalline samples as Nujol mulls) of A. $Pd(dpg)_2Br_{1.1}$, B. $Pd(dpg)_2$, C. $Ni(dpg)_2Br_{1.0}$, D. $Ni(dpg)_2$, E. (trimesic acid$\cdot H_2O)_{10}H^+Br_5^-$.

Figure 6. Electrical conductivity in the crystallographic c direction for typical $Ni(dpg)_2Br_{\nu 0}$ and $Ni(dpg)_2I$ crystals as a function of temperature.

Figure 7. Electrical conductivity (dc) in the crystallographic c direction for typical $Pd(dpg)_2Br_{\nu 1}$ and $Pd(dpg)_2I$ crystals as a function of temperature.

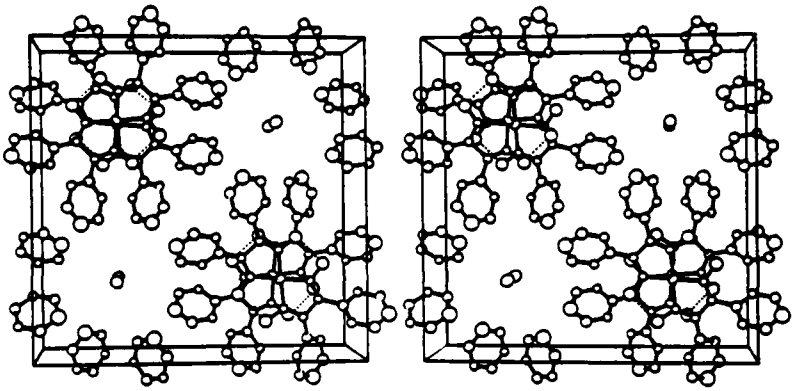

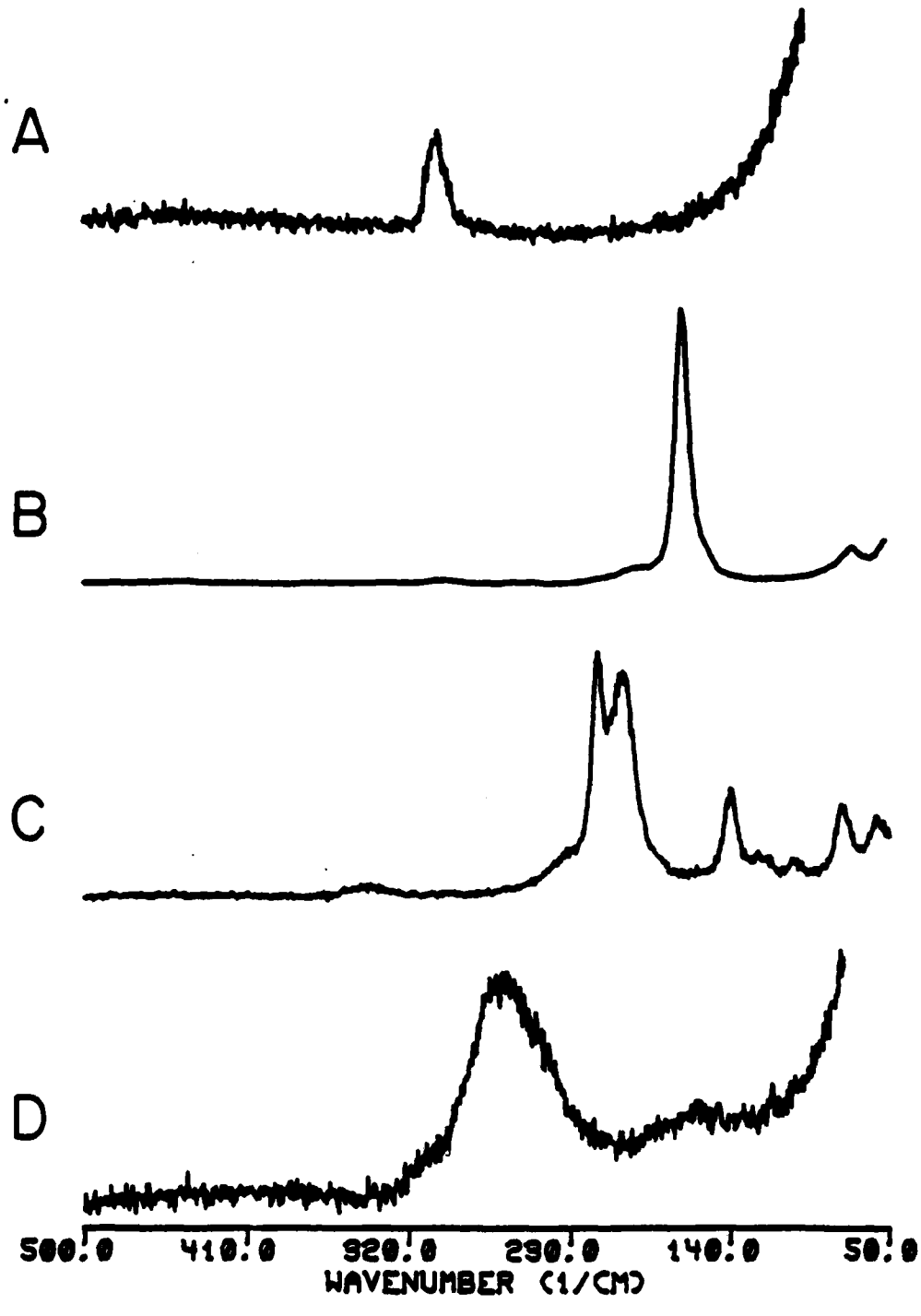
A
B
C
D
500.0
410.0
320.0
230.0
140.0
50.0
WAVENUMBER (1/CM)

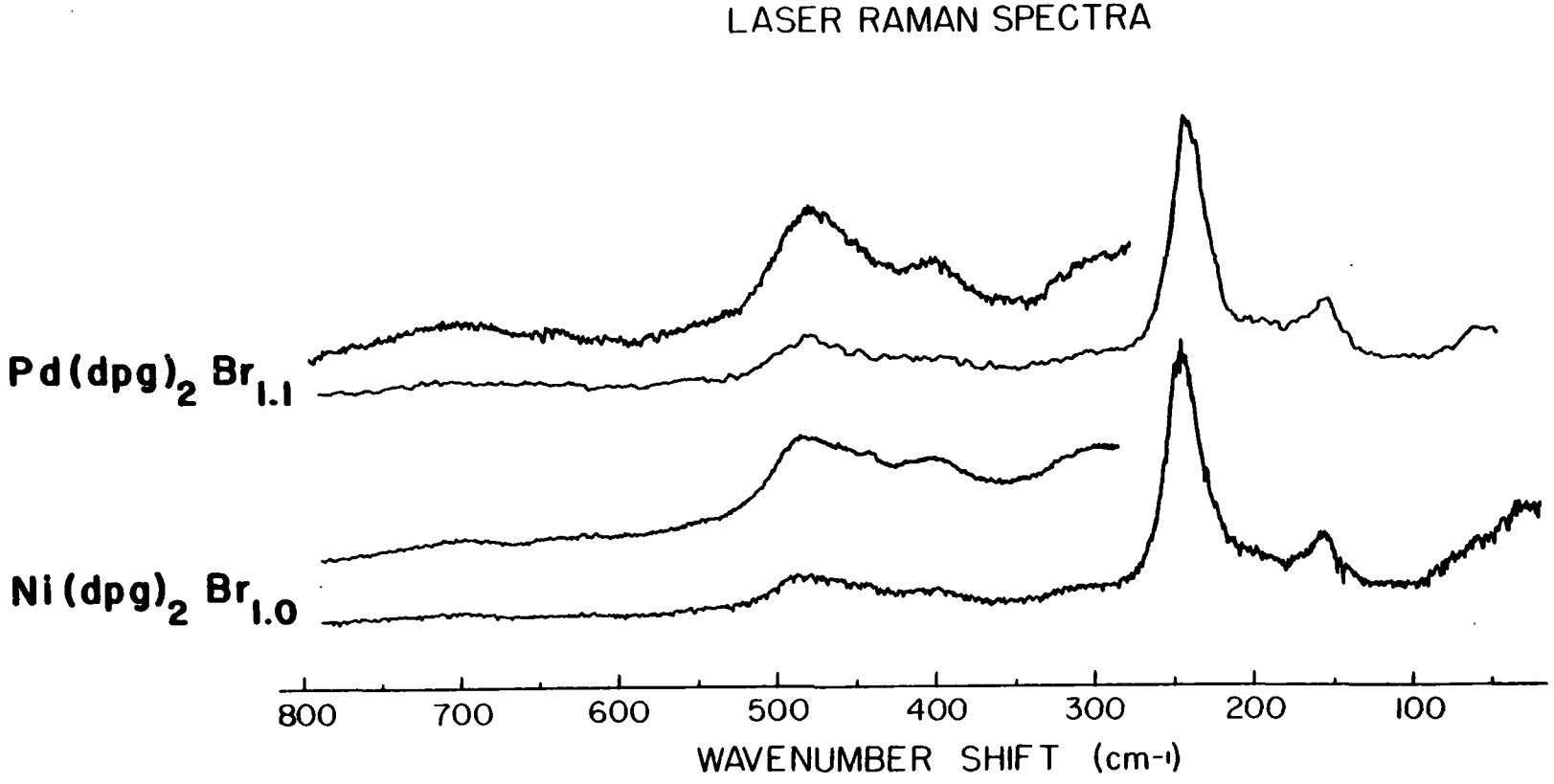
LASER RAMAN SPECTRA
Pd(dpg)2 Br1.1
Ni(dpg)2 Br1.0
800
700
600
500
400
300
200
100
WAVENUMBER SHIFT (cm-1)

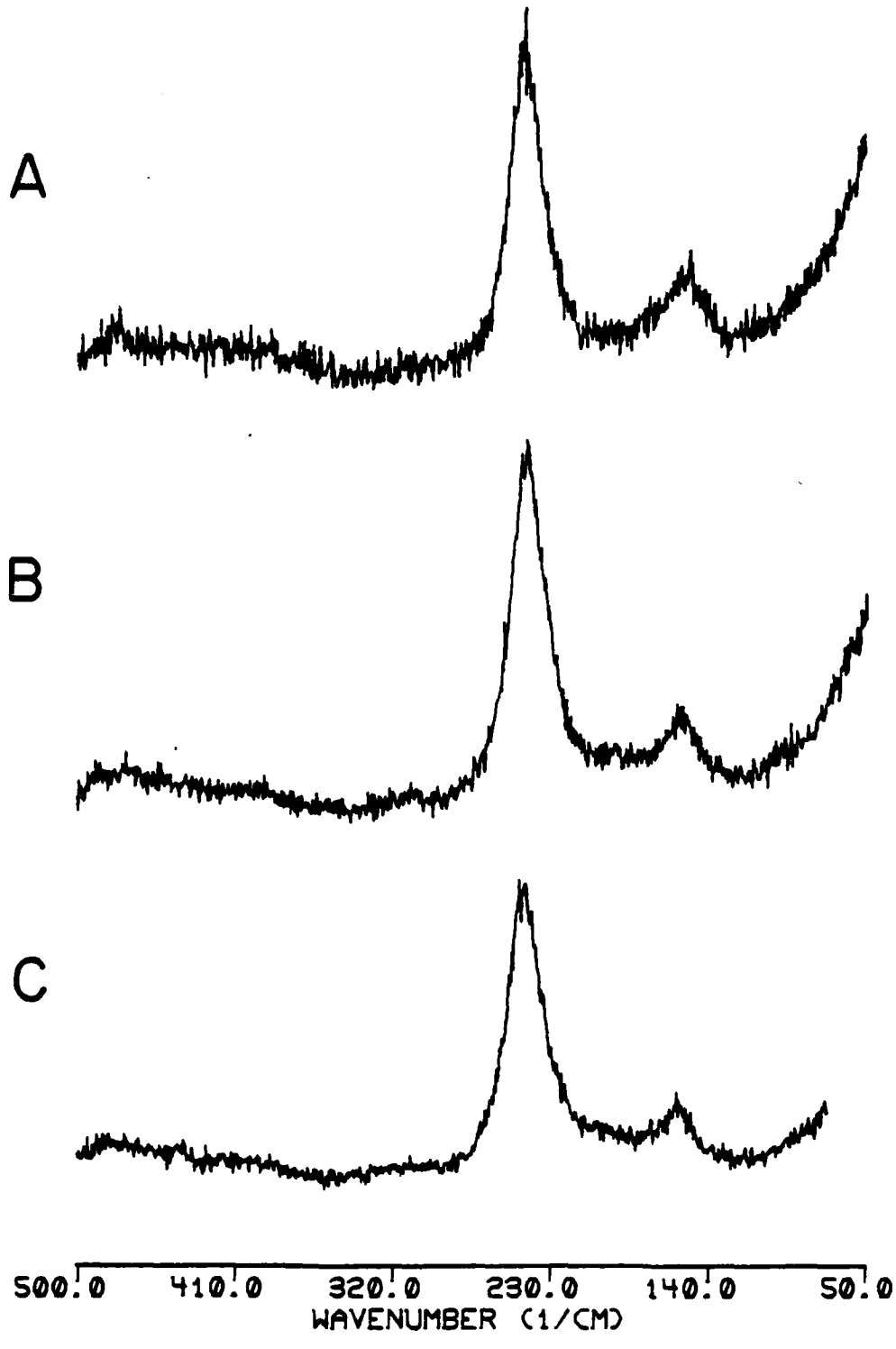
A
B
C
500.0
410.0
320.0
230.0
140.0
50.0
WAVENUMBER (1/CM)

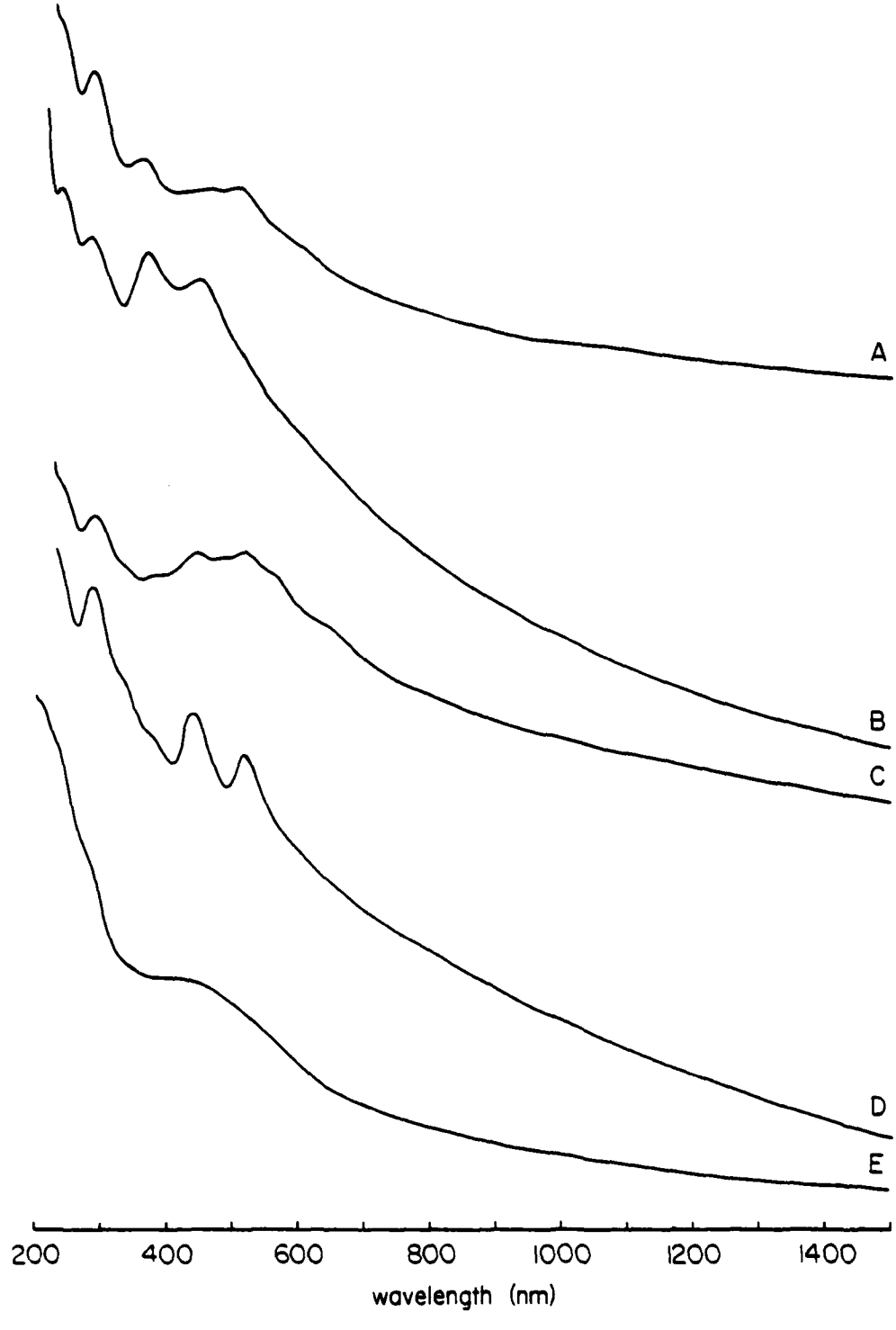
A
B
C
D
E
200
400
600
800
1000
1200
1400
wavelength (nm)

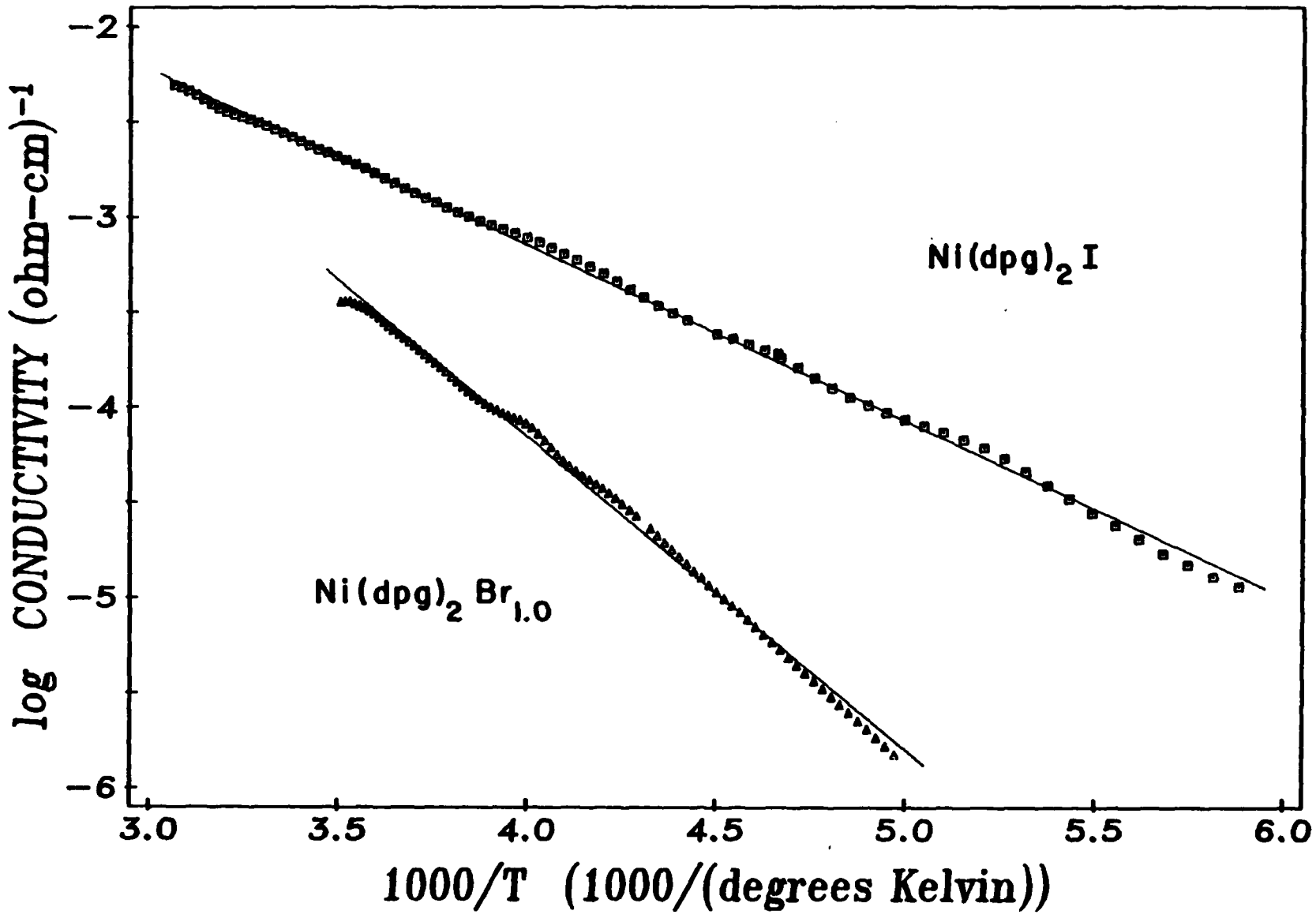
log CONDUCTIVITY (ohm-cm)$^{-1}$
−2
−3
−4
−5
−6
3.0
3.5
4.0
4.5
5.0
5.5
6.0
1000/T (1000/(degrees Kelvin))
Ni(dpg)$_2$ I
Ni(dpg)$_2$ Br$_{1.0}$

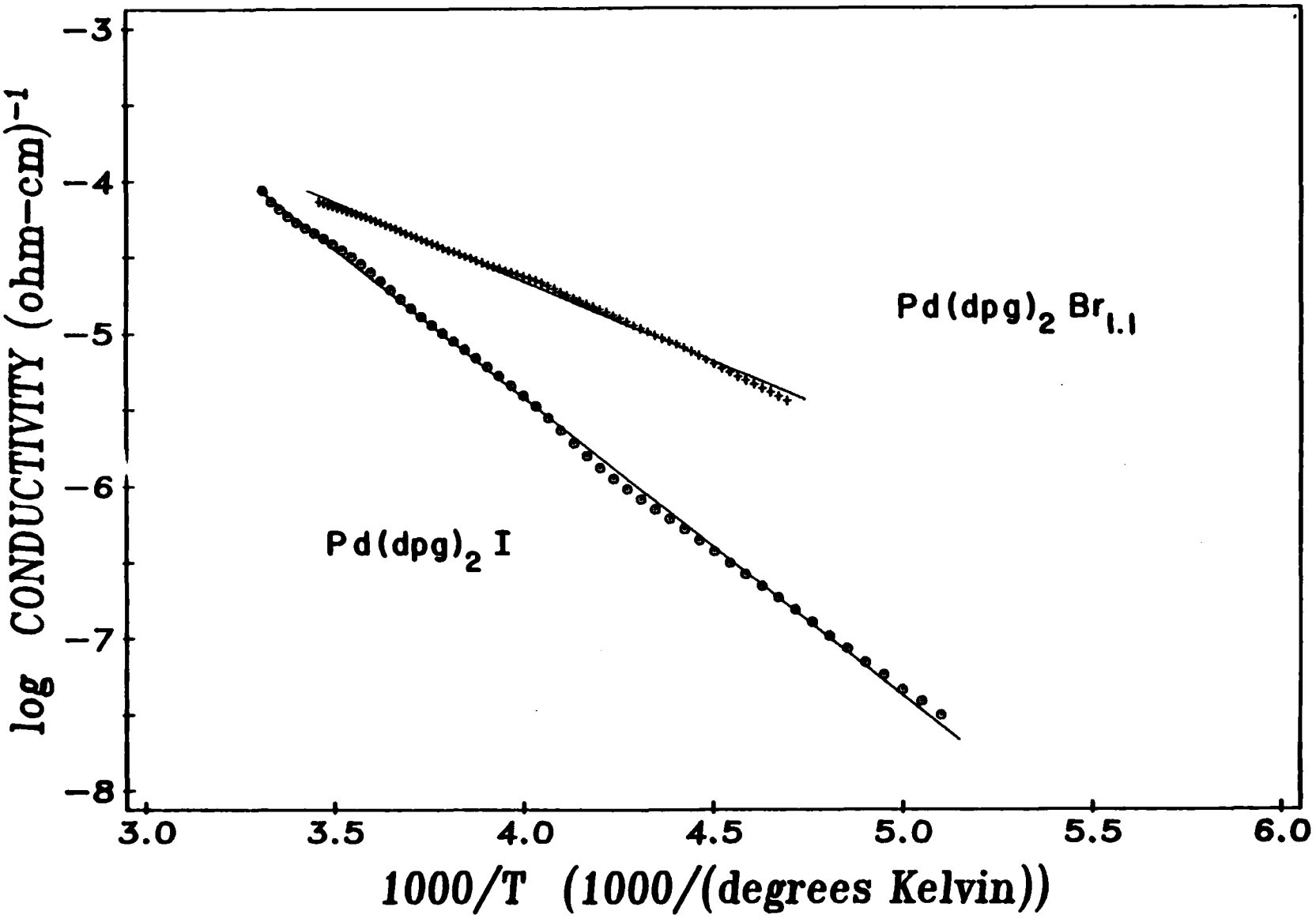
log CONDUCTIVITY (ohm-cm)$^{-1}$
-3
-4
-5
-6
-7
-8
3.0
3.5
4.0
4.5
5.0
5.5
6.0
1000/T (1000/(degrees Kelvin))
Pd(dpg)$_2$ Br$_{1.1}$
Pd(dpg)$_2$ I

P4-2/A23

472:GAN:716:tm
78u472-608

TECHNICAL REPORT DISTRIBUTION LIST, GEN

	No. Copies
Office of Naval Research Attn: Code 472 800 North Quincy Street Arlington, Virginia 22217	2
ONR Branch Office Attn: Dr. George Sandoz 536 S. Clark Street Chicago, Illinois 60605	1
ONR Branch Office Attn: Scientific Dept. 715 Broadway New York, New York 10003	1
ONR Branch Office 1030 East Green Street Pasadena, California 91106	1
ONR Branch Office Attn: Dr. L. H. Peebles Building 114, Section D 666 Summer Street Boston, Massachusetts 02210	1
Director, Naval Research Laboratory Attn: Code 6100 Washington, D.C. 20390	1
The Assistant Secretary of the Navy (R,E&S) Department of the Navy Room 4E736, Pentagon Washington, D.C. 20350	1
Commander, Naval Air Systems Command Attn: Code 310C (H. Rosenwasser) Department of the Navy Washington, D.C. 20360	1
Defense Documentation Center Building 5, Cameron Station Alexandria, Virginia 22314	12
Dr. Fred Saalfeld Chemistry Division Naval Research Laboratory Washington, D.C. 20375	1
U.S. Army Research Office Attn: CRD-AA-IP P.O. Box 1211 Research Triangle Park, N.C. 27709	1
Naval Ocean Systems Center Attn: Mr. Joe McCartney San Diego, California 92152	1
Naval Weapons Center Attn: Dr. A. B. Amster, Chemistry Division China Lake, California 93555	1
Naval Civil Engineering Laboratory Attn: Dr. R. W. Drisko Port Hueneme, California 93401	1
Department of Physics & Chemistry Naval Postgraduate School Monterey, California 93940	1
Dr. A. L. Slafkosky Scientific Advisor Commandant of the Marine Corps (Code RD-1) Washington, D.C. 20380	1
Office of Naval Research Attn: Dr. Richard S. Miller 800 N. Quincy Street Arlington, Virginia 22217	1
Naval Ship Research and Development Center Attn: Dr. G. Bosmajian, Applied Chemistry Division Annapolis, Maryland 21401	1
Naval Ocean Systems Center Attn: Dr. S. Yamamoto, Marine Sciences Division San Diego, California 91232	1
Mr. John Boyle Materials Branch Naval Ship Engineering Center Philadelphia, Pennsylvania 19112	1

TECHNICAL REPORT DISTRIBUTION LIST, GEN

	No. Copies
Dr. Rudolph J. Marcus Office of Naval Research Scientific Liaison Group American Embassy APO San Francisco 96503	1
Mr. James Kelley DTNSRDC Code 2803 Annapolis, Maryland 21402	1

472:GAN:716:abc
78u472-608

TECHNICAL REPORT DISTRIBUTION LIST, 053

	No. Copies
Dr. R. N. Grimes University of Virginia Department of Chemistry Charlottesville, Virginia 22901	1
Dr. M. Tsutsui Texas A&M University Department of Chemistry College Station, Texas 77843	1
Dr. M. F. Hawthorne University of California Department of Chemistry Los Angeles, California 90024	1
Dr. D. B. Brown University of Vermont Department of Chemistry Burlington, Vermont 05401	1
Dr. W. B. Fox Naval Research Laboratory Chemistry Division Code 6130 Washington, D.C. 20375	1
Dr. J. Adcock University of Tennessee Department of Chemistry Knoxville, Tennessee 37916	1
Dr. A. Cowley University of Texas Department of Chemistry Austin, Texas 78712	1
Dr. W. Hatfield University of North Carolina Department of Chemistry Chapel Hill, North Carolina 27514	1
Dr. D. Seyferth Massachusetts Institute of Technology Department of Chemistry Cambridge, Massachusetts 02139	1
Professor H. Abrahamson University of Oklahoma Department of Chemistry Norman, Oklahoma 73019	1
Dr. M. H. Chisholm Department of Chemistry Indiana University Bloomington, Indiana 47401	1
Dr. B. Foxman Brandeis University Department of Chemistry Waltham, Massachusetts 02154	1
Dr. T. Marks Northwestern University Department of Chemistry Evanston, Illinois 60201	1
Dr. G. Geoffrey Pennsylvania State University Department of Chemistry University Park, Pennsylvania 16802	1
Dr. J. Zuckerman University of Oklahoma Department of Chemistry Norman, Oklahoma 73019	1
Professor O. T. Beachley Department of Chemistry State University of New York Buffalo, New York 14214	1
Professor P. S. Skell Department of Chemistry The Pennsylvania State University University Park, Pennsylvania 16802	1
Professor K. M. Nicholas Department of Chemistry Boston College Chestnut Hill, Massachusetts 02167	1
Professor R. Neilson Department of Chemistry Texas Christian University Fort Worth, Texas 76129	1
Professor M. Newcomb Texas A&M University Department of Chemistry College Station, Texas 77843	1